MRS Advances (2023) 8:261–266
https://doi.org/10.1557/s43580-023-00530-4

ORIGINAL PAPER

Caustic scrubber waste converted to aluminosilicates: Structures determined by nuclear magnetic resonance

John S. McCloy[1,2] · Nicholas Stone-Weiss[2] · David L. Bollinger[1]

Received: 22 January 2023 / Accepted: 16 February 2023 / Published online: 28 February 2023

Abstract

Caustic scrubbers (CS) are proposed to aid in capture of radioiodine species in future nuclear fuel aqueous reprocessing plants. Dissolved anions in the CS will include I^-, Br^-, Cl^-, OH^-, CO_3^{2-}, NO_3^-, and NO_2^-. One path for immobilization of the high pH CS solutions is to react it with kaolinite to form aluminosilicate powders, which can subsequently be consolidated. These reaction products include primarily sodalite, an amorphous component, and minor phases such as cancrinite or zeolite Na–P. In the current work, previously reported CS aluminosilicates are characterized by ^{23}Na and ^{27}Al magic angle spinning nuclear magnetic resonance (NMR). These measurements provide insight into structure of crystalline and amorphous species previously identified by X-ray diffraction. The chemical environments probed by NMR are compared to various synthesized and natural standard materials, and ^{23}Na NMR in particular shows that many different chemical environments exist in what appears to be a mixed sodalite assemblage.

Introduction

The US Department of Energy (DOE) continues to research potential reprocessing of used nuclear fuel (UNF) and disposal pathways. One option involves aqueous reprocessing, in which fuel is chopped and dissolved in nitric acid, and gaseous fission products (e.g., ^3H, ^{14}C, ^{85}Kr, ^{129}I) are released into the dissolver off-gas [1]. Arguably the most problematic of these radionuclides is ^{129}I, having a ~ 10^7 y half-life, and thus a significant contributor to long-term dose in permanent disposal scenarios. Several proposals have been made for immobilizing ^{129}I to meet US regulatory decontamination factors (DF) [2]. The currently preferred approach is to use an aqueous caustic scrubber (CS) (achieves DF > 100) followed by a solid sorbent polishing bed for the gas going through the CS liquid, allowing the possibility to meet the required DF > 1000 and simultaneously extend the life of the sorbent beds [3].The process will result in a CS solution rich in Na^+, OH^-, $^{14}CO_3^{2-}$, and halogens, including ^{129}I. In a CS, the I_2 from the off-gas disproportionates, $3I_2 + 6OH^- \leftrightharpoons 5I^- + IO_3^- + 3H_2O$, resulting in formation of iodide and a minor concentration of iodate. The approximate composition of the CS is [4]: NaOH (0.2 M), NaI (0.03 M), NaCl + NaBr (0.1 M), Na_2CO_3 (0.6 M), $NaNO_3$ (0.03 M), $NaNO_2$ (0.06 M). Iodine, bromine, and carbon are fission products, and chlorine and nitrate/nitrite come from acids used for fuel dissolution [5].

The CS solution can be immobilized into aluminosilicate minerals cancrinite [$(Na,Ca)_8(AlSiO_4)_6(OH,CO_3)_2{\cdot}xH_2O$, x ~ 2–3] and sodalite [$Na_8(AlSiO_4)_6(OH,I,Cl,Br,NO_3)_2{\cdot}xH_2O$, x ~ 0–2] using low-temperature (~ 90 °C) aqueous techniques [6, 7]. Targeting both cancrinite and sodalite allows capture and immobilization of all the anions from the scrubber solution. Since these minerals will be generated in powder form, they must be further consolidated into monolithic waste forms. To date, both borosilicate glasses [6, 8] and $ZnO–Bi_2O_3$ borate or silicate glasses [9, 10] have been considered as binding agents. The sodalite structure consists of a connected 'cage' of tetrahedra (AlO_4 and SiO_4), incorporating various anions [2, 11]. This cage for sodalite consists of 6- and 4-membered rings. The cancrinite structure has larger micropores, notably the channel surrounded by 12-membered rings of AlO_4 and SiO_4, and also contains 6- and 4-membered rings [12]. Both structures can accommodate the same anions (e.g., I^-, Cl^-, OH^-, CO_3^{2-}, SO_4^{2-}, etc.) with the preferred structure depending on the alkali and alkaline earth metals present, the Al/Si molar ratio, and the

✉ John S. McCloy
john.mccloy@wsu.edu

[1] School of Mechanical and Materials Engineering, Washington State University, Pullman, WA, USA

[2] Materials Science and Engineering Program, Washington State University, Pullman, WA, USA

amount of water, though they frequently crystallize together [11, 13, 14].

Sodalite structures often age into cancrinite under high pH conditions [15], such as during the extraction of alumina from bauxite ore using the Bayer process [16]. In the Bayer process, chemicals remove silica from the ore, resulting in waste 'desilication products' (DSP), consisting mainly of sodalite and cancrinite with some hematite (hence colloquial 'red mud'). SiO_2 is removed from the ore at the expense of some loss of Al to the aluminosilicate DSP. Aluminosilicates precipitate initially as amorphous gels which then ripen to sodalite and eventually cancrinite depending on the solution conditions [15]. Large amounts of carbonate or calcium, large Si/Al ratios, and increased temperatures and aging times, favor cancrinite over sodalite [11, 12, 17].

In nuclear waste management, it is desirable to understand the distribution of waste anions in the structures of sodalite, cancrinite, and any remaining amorphous phases. It has been shown [7] that X-ray diffraction (XRD) is not ideal for distinguishing amongst possible phases, and it cannot be reliably determined by XRD whether the individual particles contain only one anion or multiple mixed anions. Previous work using solid state synthesis to create binary anion sodalites suggested a random mixing in (Cl,Br) and (Cl,I) sodalites, based on linear models of the lattice parameter [18]. Anion clustering in mixed sodalites has been investigated, with pertechnetate/perrhenate found not to cluster according to microscopic techniques [19], while nitrate/perrhenate do cluster according to XRD, with the nitrate incorporation being favored [20]. Studies of incorporation of perrhenate and other monovalent (chloride, nitrate, permanganate) or divalent anions (carbonate, sulfate, and tungstate) showed that anion size was the major factor in partitioning in sodalite cages with only two anions (plus water) [21]. Studies with more complex anion solutions, indicative of alkaline radioactive tank waste, showed that in the presence of hydroxide, nitrate, nitrite, and chloride—all small anions—perrhenate did not incorporate well [22]. Sodalite normally formed with nitrite, and cancrinite with nitrate [22].

Other experiments using hydrothermal synthesis, thus having also H_2O and related species compete for the cage, show a more complicated distribution, where the size requirements of the different anion species and the enthalpic differences of the sodalite cages create situations where ideal random mixing is not achieved, but rather some separation and selectivity [23]. The characterization method of choice in these studies was magic angle spinning (MAS) nuclear magnetic resonance (NMR), of cage species such as ^{35}Cl, ^{81}Br, and ^{127}I, charge compensator ^{23}Na, and framework species ^{27}Al [23]. ^{23}Na NMR was particularly useful for distinguishing multiple environments, and ^{27}Al NMR indicated the average bond angle T-O-T, where T is the tetrahedron of Si or Al [24, 25]. In the current study, we investigated the mixed sodalites produced from CS solution, using ^{23}Na and ^{27}Al MAS NMR, to gain insight into the structure of these materials.

Experiments

The synthesis conditions for the aluminosilicate powders studied here were described previously [7]. Briefly, a liquid mixture of simulated CS solution, including sodium salts of OH^-, I^-, Cl^-, Br^-, CO_3^{2-}, NO_3^-, and NO_2^- in water was created. Then a stoichiometric amount of kaolinite was added to produce sodalite. The mixtures were synthesized in either an open beaker or closed autoclave, depending on the experiment, and heated at different temperatures from 90 °C to 150 °C, for up to 7 days (for those studied here). In some cases, the NaOH/kaolinite ratio was varied. For the purposes of the current investigation, five selected CS aluminosilicate batches, of the 25 variations synthesized, were subjected to NMR, on the basis that they should show different behaviors according to their crystal phases determined from previous XRD. CS 2 was (approximate weight %) 60% sodalite, 26% amorphous, 14% kaolinite, presumably unreacted. CS 6 was 52% zeolite P, 37% sodalite, 8% amorphous, 2% kaolinite, and 1% other. CS 11 was 83% sodalite, 16% amorphous, < 1% kaolinite and cancrinite. CS 12 was 78% sodalite, 22% amorphous, and < 1% of kaolinite and cancrinite. CS 17a contained 79% sodalite, 18% amorphous, 3% cancrinite, and < 1% other.

In addition to these six CS batches, standards for ^{23}Na and/or ^{27}Al were also investigated by NMR. These included analytical grade NaOH, NaBr, NaI, and NaCl chemicals. Several zeolites were studied, including Zeolite 4A (Grace), as well as Zeolite NaP1 (Zeo-P1) and Zeolite NaP2 (Zeo-P2), synthesized as described in Parruzot et al. [26]. Carbonate cancrinite (CAN) was also synthesized, according to [17]. Three sodalites were investigated: natural chlorosodalite (Cl-SOD), as described by Chong [27]; iodosodalite (I-SOD), synthesized hydrothermally from $NaAlO_2$, colloidal SiO_2, NaI, NaOH, and H_2O, and aged at 100 °C for 20 d; and hydrosodalite (H-SOD), synthesized hydrothermally from $NaAlO_2$, colloidal SiO_2, NaOH, and H_2O, and aged at 180 °C for 2 d. The synthetic materials are described fully in supplementary information of [7].

Single resonance ^{27}Al and ^{23}Na MAS NMR spectra were recorded on a 14.1 T Varian DD2 600 MHz spectrometer using a 4.0 mm probe (Agilent). Powdered samples were packed into 4.0 mm zirconia rotors and spun at 10 kHz. ^{27}Al MAS NMR spectra were measured at 156.27 MHz with $\pi/6$-pulse durations of 0.8–1.7 μs and recycle delays of 1 s. ^{23}Na MAS NMR spectra were measured at 158.63 MHz with $\pi/6$-pulse durations of 1.3–1.5 μs and recycle delays of 0.5–1 s. Measurements were signal-averaged over at least

100 scans and processed without line broadening. ^{27}Al shifts were reported relative to powdered $AlPO_4$—measured at 40.7 ppm relative to aqueous 1 M $Al(NO_3)_3$; ^{23}Na shifts were reported relative to powdered NaCl—measured at 7.2 ppm relative to aqueous 0.1 M NaCl.

A ^{23}Na z-filtered Multiple-Quantum MAS (MQMAS) NMR experiment was performed at 14.1 T on the CS 12 sample, using a standard three-pulse sequence [28]. Hard pulses of 6.0–7.2 µs and 2.2–2.4 µs for multi-quantum excitation and reconversion, respectively, and a third soft detection pulse of 10 µs. Recycle delays of 1 s were used and the t_1 evolution period consisted of 64 increments of 20–40 scans each. The reconversion and selective pulses were spaced with a z-filter of 10 µs duration. One-dimensional ^{23}Na MAS NMR spectra of all the CS samples were fitted using Gaussian/Lorentzian and CzSimple models in DMFit, guided by the findings from MQMAS NMR results.

Results and discussion

Results for the ^{27}Al investigation are shown in Fig. 1a. The major resonance for all tested samples was a peak 59–65 ppm, indicating tetrahedral aluminum, i.e., Al (IV), coordinated by oxygen atoms [29]. Since ^{27}Al is a quadrupolar nucleus, the peak maximum does not directly correspond to the isotropic chemical shift. There is evidence of a small amount of octahedral aluminum, Al (VI), in CS 2 and CS 6, likely due to residual kaolinite, in agreement with XRD.

The main signal (Fig. 1b) is the Al (IV) as expected from tectosilicates like sodalite, cancrinite, and zeolites. In these aluminosilicates, the topology has Al (IV) alternately connected to Si (IV) by vertex shared tetrahedra in *n*-member rings of 4 or 8 (Zeolite NaP, gismondine (GIS) framework), 4, 6, or 8 (Zeolite 4A, Linde Type A (LTA) framework), 4 or 6 (sodalite, SOD framework), or 4, 6, or 12 (cancrinite, CAN

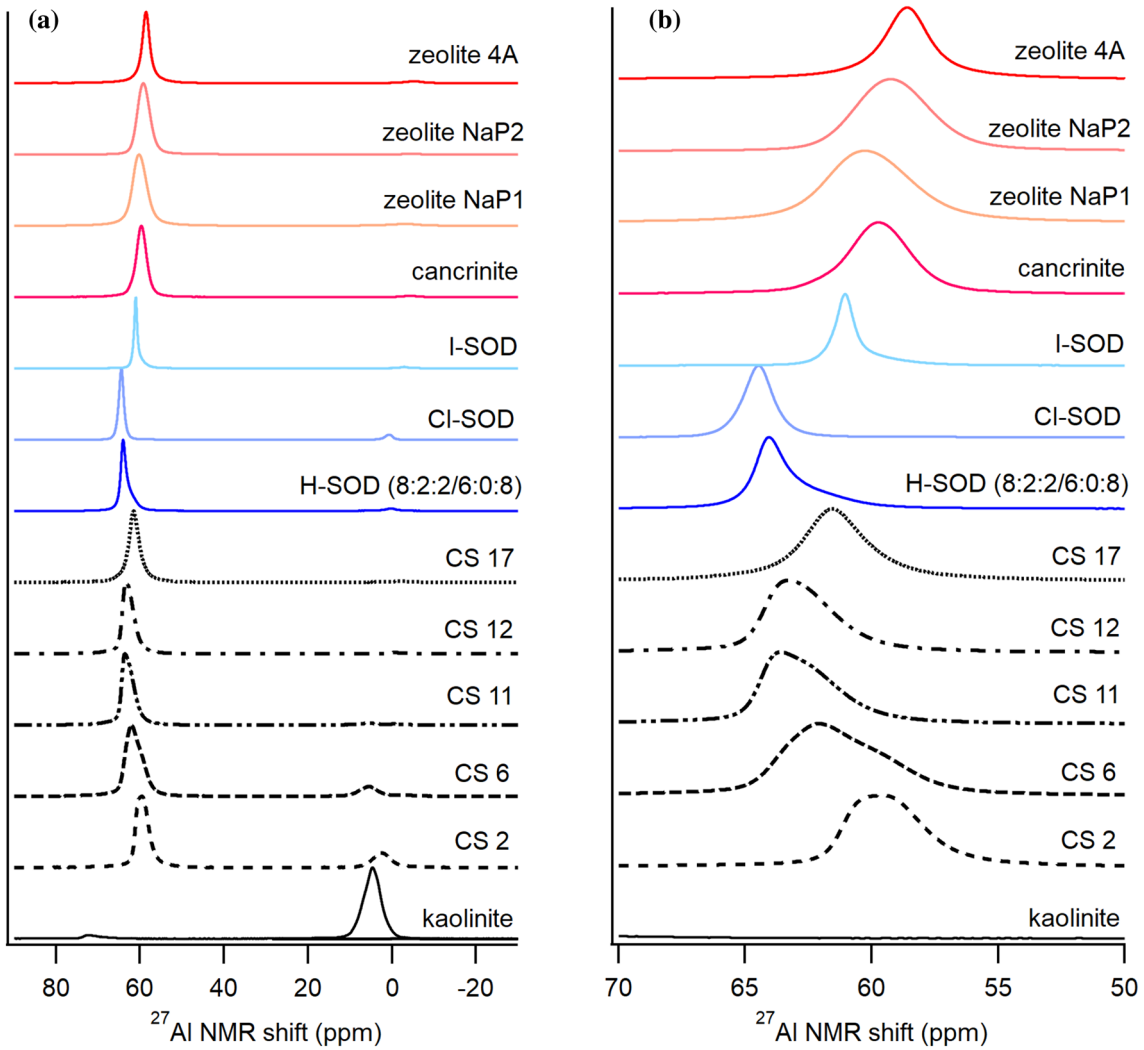

Fig. 1 ^{27}Al MAS NMR spectra, **a** showing Al(IV) and Al(VI) species and **b** close-up of the Al(IV) region

framework). Some details of the Al (IV) resonance chemical shift and linewidth depends on the precise chemical environments of the Al(IV) atoms, and is thus a sensitive indicator. The full-width half maximum (FHWM) of the measured Al (IV) resonances varies from ~ 1 ppm for iodosodalite (I-SOD) to ~ 3 ppm for Zeolite NaP2, the latter indicating a disordered structure or a deviation from spherical symmetry. For the CS samples, the Al (IV) resonance is very asymmetric, with an approximate FWHM of ~ 5 ppm for CS 6. This asymmetry could be due to second order quadrupolar effects, still present for the quadrupolar ^{27}Al even at the ~ 14 T magnetic field; additionally, multiple sites and a disordered structure would also increase the asymmetry due to a deviation from spherical symmetry. In general, the Al (IV) resonances are narrowest for the sodalites (I-SOD, Cl-SOD, H-SOD), then broader for the zeolites and CAN, and broadest for the CS samples. The CAN chemical shift is lower than the SOD chemical shifts, as has been previously observed [30]. The ^{27}Al resonance for CS 17 is similar to that recently observed for synthetic desilication products (DSP) which were found by XRD as ~ 50% sodalite, ~ 34% amorphous, ~ 13% cancrinite, and ~ 3% kaolinite [16]. The isotropic chemical shift for ^{27}Al can be related to the bond angles and mean distances between the tetrahedral atoms, as well as the next-nearest neighbor identities [29].

Results for the ^{23}Na MAS NMR investigation are shown in Fig. 2a. The shape of the ^{23}Na resonances varied considerably. ^{23}Na is also a quadrupolar nucleus, so its peak position is not identical to the isotropic chemical shift [29]. Resonances of the halide salts are narrow and single peaked, similar to those previously reported [31], with the exception of NaI which shows a weak broad feature at ~ 5 ppm, which may be due to a hydrated component of the hygroscopic salt. NaOH shows a very complicated pattern, likely due to a mix of hydration states [32, 33]. For the zeolites, the peak ranges from − 1.0 ppm for Zeolite 4A to − 4.9 ppm for Zeolite NaP2; the resonance for Zeolite NaP1 is considerably broader than the other zeolites. Cl-SOD gives a narrow resonance, while I-SOD shows multiple features, the one 6.5–3.9 ppm likely being two features of a single quadrupole site. The H-SOD spectrum is indicative of two different materials. The peak at − 3 ppm is assigned to a "6:0:8" hydrated non-basic hydrosodalite—$Na_6(AlSiO_4)_6{\cdot}8H_2O$-and the ~ 4 ppm to the "8:2:2" hydroxysodalite—$Na_8(AlSiO_4)_6(OH)_2{\cdot}2H_2O$-as described by Engelhardt et al. [34], noting that these authors used a previous convention of referencing solid NaCl to 0 ppm. The 6:0:8 H-SOD is known to form on washing, where NaOH is exchanged for H_2O in the cage [34]. For the CS materials, the main resonance is similar to that observed for CAN in the current study and for DSP in [16].

CS 12 was investigated with ^{23}Na MQMAS NMR, and five key peaks were identified (Fig. 2b). The fitting parameters are shown in Table 1. These parameters were used to

Table 1 ^{23}Na MQMAS fit for CS 12

Peak #	δ_{iso}(calc), ppm	δ_{iso}(fit), ppm	CQ(fit)	Area (%)
1	16.31	15.90	1.77	7.0
2	7.60	6.80	1.00	12.4
3	2.84	2.40	0.00	10.5
4	0.32	− 0.30	1.50	66.2
5	− 4.08	− 8.50	1.60	4.0

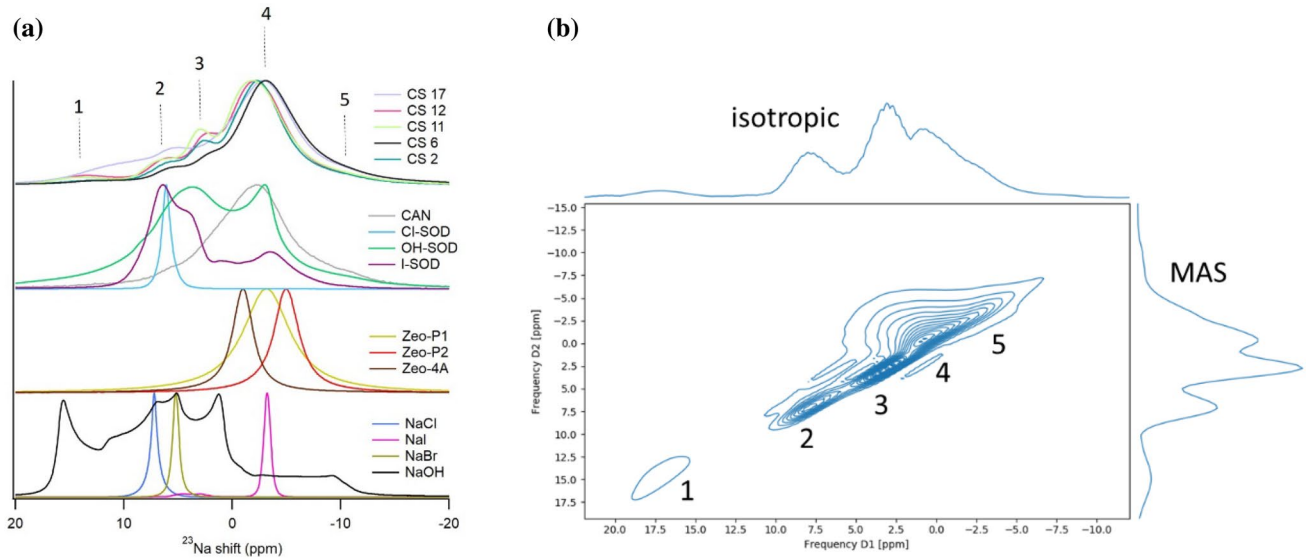

Fig. 2 ^{23}Na NMR spectra of CS and standards, **a** MAS NMR; **b** MQMAS for CS 12

guide the fitting of ^{23}Na single pulse MAS NMR spectra (Fig. 3). The main peak is #4, which in comparison to the standards (Fig. 2a) is most similar in position to CAN, Zeo-P1, and H-SOD (6:0:8). Dehydrated zeolites are known to have very broad ^{23}Na resonances due to overlapping 2nd order quadrupolar peaks at unique Na sites [29, 33]. Low symmetry sites, in both dehydrated zeolites and amorphous regions, are expected to have broad ^{23}Na resonances [35], similar to glasses and inorganic aluminosilicate polymers [36]. Thus, broad resonances can indicate either low symmetry crystalline structure or amorphous structure, or some combination. Despite the difference in position of this main peak from the SOD standards (Fig. 2a), the fact that the position and FWHM is quite similar to DSP [16], known to be comprised of a SOD + CAN + amorphous phase assemblage, suggests that this peak in CS can be similarly identified. The identity of the other peaks could not be determined unambiguously.

The broadness of the central CS peak may be attributable to unique Na sites as well as anionic disorder. For example, in CAN, which remains hydrated, the assumed anionic distribution disorder of CO_3^{2-} and OH^- may lead to broadening. Similarly, for the H-SOD, disorder of OH^- and $H_3O_2^-$ in the cage may broaden the ^{23}Na signal. By contrast, in the case of Zeolite Na–P1, there are multiple crystallographic Na sites even without anion disorder, while in CAN there are multiple Na sites [37] in addition to anion disorder.

From the standpoint of waste management, the most important factor is the immobilization of the waste components, and their stability in the final waste form. The strategy of incorporating anions into crystalline structures, such as cages in aluminosilicates, in principal results in increased thermodynamic stability compared to such anions embedded in an amorphous phase. The question of whether it is better to have random anion distribution, non-random distribution, or physical mixture of distinct phases is a more complicated one, but can be potentially answered by future thermodynamic studies. Presumably, the randomly mixed anion structure would reflect a weighted averaged enthalpic stability from their constituent anion cages, while also gain entropic stability based on configurational entropy due to the ideal mixing. The non-random distribution of anion (but single phase) may have further enhanced enthalpic stability (to be confirmed with future thermodynamic studies). Moreover, besides structural-related stability, some sodalites, for instance, have been shown to be stabilized by a considerable content of water (which may be chemically sorbed and thus provide strong thermodynamic stabilization of the phase), and some anion exchange may be favored for certain anions after formation in mixed anion liquids [38]. Specific thermodynamic studies of carefully controlled deliberately mixed sodalites are needed to assess the relative stability of mixed anion systems versus end members. Until these data are available, it is not easy to say whether single phase mixed cage aluminosilicates or multiple phase single anion aluminosilicates would be preferred for waste management.

Conclusions

Overall, this study broadly assessed the structure of aluminosilicates produced from simulated caustic scrubber solution, having a variety of possible anions to fill the cages of sodalite, cancrinite, zeolite, and related materials. The observed broad central ^{23}Na peak in CS materials suggests both anion or structural disorder and some 2nd order quadrupolar broadening due to similar but slightly different Na sites. It is likely that the anions are distributed non-randomly, given

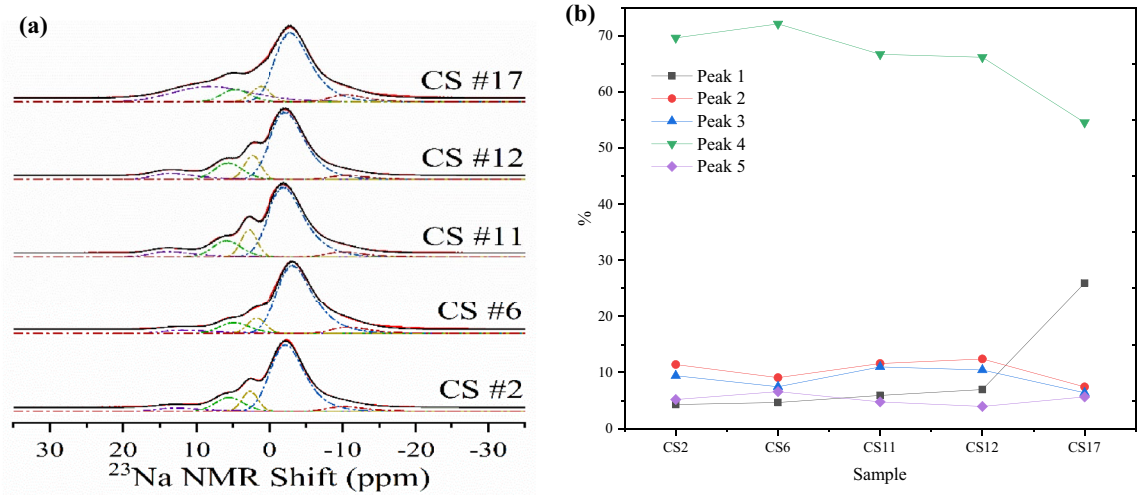

Fig. 3 ^{23}Na NMR fitted spectra of CS materials, **a** fits; **b** area fraction

the presence of minor ^{23}Na signatures in addition to the main broad peak in ^{23}Na MAS NMR. This is supported by the ^{27}Al MAS NMR, which shows asymmetric Al(IV) peaks suggesting multiple species. While these individual SOD or similar structure phases cannot be individually identified, this study shows the value of NMR in assessing the structure of complex aluminosilicate mixtures containing non-trivial quantities of amorphous phase. The fact that all the CS ^{23}Na spectra are so alike confirms a broadly charge-compensating role and similar structural role for these ions regardless of the specific crystal structure. The ^{27}Al signature, on the other hand, does indicate a somewhat narrower and more symmetric resonance for the CS 17a which has the highest SOD and lowest amorphous content, per XRD. Apparently, in this case the ^{27}Al NMR is more telling than the ^{23}Na spectra.

Acknowledgments The authors acknowledge support from the United States Department of Energy (US DOE) Office of Nuclear Energy (DE-NE0008964). Thanks to Natalie Smith-Gray and Andy Lipton for a few of the NMR measurements, Saehwa Chong for cancrinite synthesis, Brian Riley for providing the zeolite NaP samples, and Ashutosh Goel, Xiaofeng Guo, and Dan Gregg for helpful discussions.

Data availability The data that support the findings of this study are available from the corresponding author upon reasonable request.

Declarations

Conflict of interest The authors declare no known conflicts of interest.

References

1. J.D. Vienna, E.D. Collins, J.V. Crum, W.L. Ebert, S.M. Frank, T.G. Garn, D. Gombert, R. Jones, R.T. Jubin, V.C. Maio, J.C. Marra, J. Matyas, T.M. Nenoff, B.J. Riley, G.J. Sevigny, N.R. Soelberg, D.M. Strachan, P.K. Thallapally and J.H. Westsik, Closed Fuel Cycle Waste Treatment Strategy, Idaho National Laboratory, Idaho Falls, ID, INL/EXT-15–34504, PNNL-24114 (2015)
2. B.J. Riley, J.D. Vienna, D.M. Strachan, J.S. McCloy, J.L. Jerden Jr., J. Nucl. Mater. **470**, 307 (2016)
3. R.T. Jubin, S.H. Bruffey and J.A. Jordan, Testing of an Integrated Iodine Scrubber and Polishing Bed System, Oak Ridge National Laboratory, Oak Ridge, TN, ORNL/TM-2018/1000; NTRD-MRWFD-2018–000195 (2018)
4. R.T. Jubin, Composition of caustic scrub solution, Personal communication to: DOE NEUP program, 13 Aug 2019 (2019)
5. R.T. Jubin, Design and Test Plan for an Integrated Iodine Scrubber and Polishing Bed System, Oak Ridge National Laboratory, Oak Ridge, TN, ORNL/SR-2017/564; NTRD-MRWFD-2018–000209 (2017)
6. J. Nam, S. Chong, B.J. Riley, J.S. McCloy, MRS Adv. **3**, 1093 (2018)
7. D.L. Bollinger, J. Erickson, J.M. Bussey, J.S. McCloy, MRS Adv. **7**, 110 (2022)
8. S. Chong, J.A. Peterson, B.J. Riley, D. Tabada, D. Wall, C.L. Corkhill, J.S. McCloy, J. Nucl. Mater. **504**, 109 (2018)
9. T.J. Garino, T.M. Nenoff, J.L. Krumhansl, D.X. Rademacher, J. Am. Ceram. Soc. **94**, 2412 (2011)
10. A.J. Lere-Adams, N. Stone-Weiss, D.L. Bollinger, J.S. McCloy, MRS Adv. **7**, 90 (2022)
11. S. Chong, J. Peterson, J. Nam, B. Riley, J. McCloy, J. Am. Ceram. Soc. **100**, 2273 (2017)
12. G.D. Gatta, P. Lotti, Am. Miner. **101**, 253 (2016)
13. A.R. Gerson, K. Zheng, J. Cryst. Growth **171**, 209 (1997)
14. Y. Deng, M. Flury, J.B. Harsh, A.R. Felmy, O. Qafoku, Appl. Geochem. **21**, 2049 (2006)
15. M.C. Barnes, J. Addai-Mensah, A.R. Gerson, Microp. Mesop. Mater. **31**, 287 (1999)
16. D.L. Bollinger, J. Erickson, N. Stone-Weiss, A.J. Lere-Adams, S. Karcher, I.D. Akin, J.S. McCloy, Environ. Adv. **6**, 100136 (2021)
17. K. Hackbarth, T.M. Gesing, M. Fechtelkord, F. Stief, J.C. Buhl, Microp. Mesop. Mater. **30**, 347 (1999)
18. M.T. Weller, G. Wong, Eur. J. Sol. State Inorg. Chem. **26**, 619 (1989)
19. E.M. Pierce, K. Lilova, D.M. Missimer, W.W. Lukens, L. Wu, J. Fitts, C. Rawn, A. Huq, D.N. Leonard, J.R. Eskelsen, B.F. Woodfield, C.M. Jantzen, A. Navrotsky, Env. Sci. Technol. **51**, 997 (2017)
20. J.O. Dickson, J.B. Harsh, M. Flury, W.W. Lukens, E.M. Pierce, Environ. Sci. Technol. **48**, 12851 (2014)
21. J.O. Dickson, J.B. Harsh, W.W. Lukens, E.M. Pierce, Chem. Geol. **395**, 138 (2015)
22. J.O. Dickson, J.B. Harsh, M. Flury, E.M. Pierce, Microp. Mesop. Mater. **214**, 115 (2015)
23. H Trill, Sodalite Sold Solution Systems: Synthesis, Topotactic Transformations, and Investigation of Framework-Guest and Guest-Guest Interactions, Doctoral disseration, Westfälischen Wilhelms-Universität Münster (2002)
24. H. Trill, H. Eckert, V.I. Srdanov, J. Am. Chem. Soc. **124**, 8361 (2002)
25. H. Trill, H. Eckert, V.I. Srdanov, J. Phys. Chem. B **107**, 8779 (2003)
26. B. Parruzot, J.V. Ryan, J.L. George, R.K. Motkuri, J.F. Bonnett, L.M. Seymour, M.A. Derewinski, J. Nucl. Mater. **523**, 490 (2019)
27. S. Chong, *Characterization of Sodalite Based Waste Forms for Immobilization of ^{129}I, Materials Science and Engineering, PhD dissertation* (Washington State University, Washington, 2017)
28. J.-P. Amoureux, C. Fernandez, S. Steuernagel, J. Magn. Reson. Ser. A **123**, 116 (1996)
29. K.J.D. MacKenzie, M.E. Smith, *Pergamon Multinuclear Solid-State Nuclear Magnetic Resonance of Inorganic Materials* (Elsevier, Pergamon, 2002)
30. N.D. Pahlevi, B. Guo, K. Sasaki, Ceram. Inter. **44**, 8635 (2018)
31. R.E.J. Sears, J. Chem. Phys. **66**, 5250 (1977)
32. H. Koller, G. Engelhardt, A.P.M. Kentgens, J. Sauer, J. Phys. Chem. **98**, 1544 (1994)
33. S.F. Dec, G.E. Maciel, J.J. Fitzgerald, J. Amer. Chem. Soc. **112**, 9069 (1990)
34. G. Engelhardt, J. Felsche, P. Sieger, J. Am. Chem. Soc. **114**, 1173 (1992)
35. S. Hayashi, K. Hayamizu, O. Yamamoto, Bull. Chem. Soc. Jpn. **60**, 105 (1987)
36. M.R. Rowles, J.V. Hanna, K.J. Pike, M.E. Smith, B.H. O'Connor, Appl. Magn. Res. **32**, 663 (2007)
37. H.D. Grundy, I. Hassan, Canad. Mineral. **20**, 239 (1982)
38. K. Lilova, E.M. Pierce, L. Wu, A.M. Jubb, T. Subramani, A. Navrotsky, ACS Earth Space Chem. **4**, 2153 (2020)